

Geometric Foraging Strategies in Multi-Agent Systems Based on Biological Models

Musad Haque, Amir Rahmani, and Magnus Egerstedt

Abstract—In nature, communal hunting is often performed by predators by charging through an aggregation of prey. However, it has been noticed that variations exist in the geometric shape of the charging front; in addition, distinct differences arise between the shapes depending on the particulars of the feeding strategy. For example, each member of a dolphin foraging group must contribute to the hunt and will only be able to eat what it catches. On the other hand, some lions earn a “free lunch” by feigning help and later feasting on the prey caught by the more skilled hunters in the foraging group. We model the charging front of the predators as a curve moving through a prey density modeled as a reaction-diffusion process and we optimize the shape of the charging front in both the free lunch and no-free-lunch cases. These different situations are simulated under a number of varied types of predator-prey interaction models, and connections are made to multi-agent robot systems.

I. INTRODUCTION

Social animals often resort to communal hunting techniques to increase their chances of catching prey and one common approach is to charge through the aggregation of prey. Bottlenose dolphins, *Tursiops truncatus*, and African lions, *Panthera leo*, are examples of biological systems that utilize such foraging methods. These predators arrange themselves in a specific formation to create a predator front that moves together, in unison, towards the collection of prey. However, the shape of the dolphin fronts are different from those of lions and this difference can be attributed to the nature of their feeding strategies, e.g., [1], [2]. Our goal is to recover these differences by optimizing over the shape of the front for a given feeding strategy.

Each member of the dolphin foraging group must contribute in the hunt [1]; on the other hand, most lions in the group feast on the prey caught by others in the group [2]. In this paper, we optimize predator fronts for foraging multi-agent systems by drawing inspiration from these two biological systems as representatives of two distinct cases: the *free lunch* (lion-inspired) and the *no-free lunch* case (dolphin-inspired). The predator front is modeled as a quadratic curve and the total energy intake of the agents over the curve and the energy of the agent that accumulates the least energy is calculated under varied types of predator-prey interaction models. The free lunch curve maximizes the total energy

intake and the no-free lunch curve maximizes the energy of the agent that feeds the least.

A potential application for prescribing the geometric shape of a charging front of foraging robots is the US Navy Sea shield mission, in which teams of autonomous vehicles will coordinate with each other to secure littoral regions [3]. Threats in the littoral regions usually consist of mines, submarines, and unmanned underwater vehicles (UUVs), which must be neutralized before other teams can land on shore. With such engineering applications as the back-end of our bio-inspired work, we design the predator fronts by developing a simple, yet expressive model of the biological systems, where the simplicity of the the model allows it to be implemented in engineered devices, such as a multi-agent robot system. At the same time, the model will be rich enough to replicate complex biological phenomena (e.g., the capturing of prey).

The foraging task is of eminent interest to the multi-robot community (for a representative sample, see [4], [5], [6], [7], [8]); yet previous work primarily focuses on the search and retrieval aspects of foraging stationary objects or cooperative agents. In [4], the effects of physical interference is presented for different foraging strategies, such as the “bucket brigading strategy,” where each robot is in charge of a sub-area of the entire foraging region. The effects of behavioral diversity of the foraging group is studied in [5], where the behaviors range from “homogeneous” to “specialized.” Bio-inspired foraging strategies, based on ants and bees, are presented in [6] and [7], respectively. In this work, for a given feeding strategy, we obtain the most efficient predator front through the solution to an optimization problem.

The remainder of the paper is organized as follows: Section II describes, in detail, the two types of biological systems under consideration. Our curve-based model of the charging front is presented in Section III and the prey movement rules are prescribed in Section IV. In Section V, we describe how we obtain the free lunch and the no-free lunch curves. Simulation results are provided in Section VI along with discussions in Section VII. Finally, Section VIII presents the conclusions.

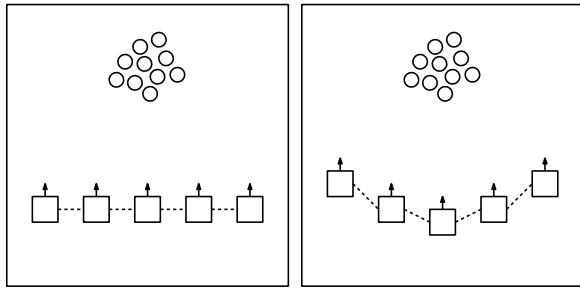
II. BIOINSPIRATION

Here, we discuss the foraging techniques of the two biological systems, Bottlenose dolphins and African lions, which serve as inspiration for our multi-agent cooperative foraging strategy.

Dolphins exhibit sophisticated coordination as a group while searching for food and capturing prey. Dolphins have

This work was supported by The Office of Naval Research through MURI-HUNT

M. Haque, A. Rahmani, and M. Egerstedt are with the School of Electrical and Computer Engineering, Georgia Institute of Technology, Atlanta, GA 30332, U.S.A. {musad.haque, amir.rahmani, magnus}@ece.gatech.edu



(a) Dolphins driving in a “line abreast” formation. (b) Lions driving in a “catcher’s mitt” formation.

Fig. 1. The arrangement of foragers in the predator front is shown for dolphins and lions. Predators (squares) are driving towards (arrows) the direction of their prey (circles).

several prey capturing techniques at their disposal and the particular method we are interested in is known as the *wall method* (for details, see [1]). In this method, dolphins arrange themselves next to each other to create a front that charges through a school of fish, as shown in Fig. 1a. The shape of the front is described in [1] as being “line abreast” and the usefulness of the method stems from the ability of this shape to constrict the movement of the fish. Moreover, each dolphin contributes in the hunt and only eats what it can catch.

Interestingly, African lions, another social animal, implement a prey capturing technique quite similar to the wall method. When hunting medium-sized prey like zebra, a single lion has a low success rate (about 17%) [2] and as a result, lions revert to group hunting and one technique that is often used is very similar to the wall method. Female lions are usually in charge of foraging and while charging towards their prey, lionesses in the “wing” positions cause the prey to drive towards the lionesses waiting in the “center” positions [9]. The resulting predator front that drives towards the prey is therefore *U-shaped*, often described as a “catcher’s mitt” [2] as shown in Fig. 1b. A zebra typically weighs around 250 kg and although it is brought down by a single lion, others in the group claim their share and earn a free lunch.

We draw inspiration from these two different social animals that use a similar idea during communal hunting to prescribe efficient curves. In the next section, we present our model of the predator front based on curve deformation techniques.

III. PREDATOR FRONT AS CURVES

Our goal is to find the most efficient curves for 1) the free lunch and 2) the no-free lunch case. In a related work, Zhang *et al.* [10] proposed a control law for mobile particles to converge to predefined spatial patterns. In another related work, Lankton *et al.* [11] use a curve evolution technique for image segmentation. There, based on the optimality condition on the speed of the curve, a gradient descent algorithm is used to deform the shape of the curve and detect objects. Since our goal is to develop simple biological models that can be implemented on engineered systems, to

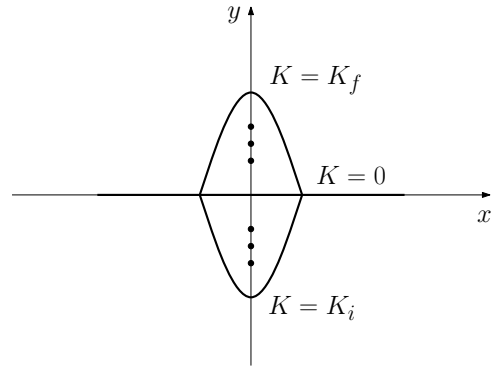


Fig. 2. The curves are parameterized by K and the candidate curves being swept through the aggregation of prey include all the curves between $K = K_i$ and $K = K_f$.

identify the most efficient curves, we specify a candidate set of curves *a priori*, and each curve from this candidate set is swept through the aggregation of prey.

More specifically, we only consider quadratic curves, where each candidate curve has the same arc length. The constant arc length requirement is placed from an engineering design perspective. If our multi-agent system consists of M agents, each with a limited communication range, it is desirable to restrict inter-agent distances to remain within this range so that each agent remains in constant communication with its neighboring agents. Since our predator agents create a front and charge towards the prey while maintaining the shape of the front, we simply require all of the candidate curves to be of the same arc length, L ; thus if we have M agents, the inter-agent arc length remains $\frac{L}{M-1}$.

Consider the curve of the form $y = ax^2 + K$ and arc length L . In fact, due to the constant length assumption, the coefficient a depends on K . More specifically, if the endpoint of the curves are $(-x_m, 0)$ and $(x_m, 0)$, where $x_m > 0$, then the K -parametrized curve, $C(K)$, is given by

$$y = \frac{-K}{x_m^2}x^2 + K, \quad (1)$$

where, x_m is given by solving the following equation:

$$\begin{aligned} L &= \int_{-x_m}^{x_m} \sqrt{1 + \frac{dy}{dx}} dx \\ &= \int_{-x_m}^{x_m} \sqrt{1 + \frac{-2K}{x_m^2}x} dx. \end{aligned} \quad (2)$$

This formulation gives us the shape of the candidate curve for each value of K . If the candidate curves under consideration include all curves between $C(K_i)$ and $C(K_f)$, then we can denote the set of candidate curves as $\mathcal{C} = \{C(K) \mid K \in [K_i, K_f]\}$, as shown in Fig. 2.

Each K -parametrized curve charges towards the prey aggregation and if we assume, without loss of generality, that the front charges in the direction of increasing y , from $t = 0$ to $t = t_f$ with a speed v_c , then at time t , the curve $C(k)$ is given by $y = \frac{-K}{x_m^2}x^2 + K + v_c t$.

IV. PREY AGGREGATION AS A DENSITY FUNCTION

The 2D prey density is denoted by $u(x,y,t)$, where $u : \mathbb{R}^2 \times \mathbb{R} \rightarrow \mathbb{R}$ and (x,y) represents Cartesian coordinates. We consider two types of processes to define prey movement, which in turn describes our predator-prey interaction, one is a simple diffusion and the other is a reaction-diffusion. Representing prey as a density function and using reaction-diffusion equations to model the spatio-temporal profile of prey is formally known as the ‘‘population framework’’ to model prey [12]. We use this approach, as opposed to an agent-based model of prey, such as the one presented in [13], as we are interested in the collective movement of prey, whereas the agent-based approach requires us to define control laws for the movement of individual prey-like agents. The details of our movement laws are discussed in more detail below.

A. Diffusion

The first type of prey movement is a diffusion given by

$$\frac{\partial u(x,y,t)}{\partial t} = v_0 \left(\frac{\partial^2 u(x,y,t)}{\partial x^2} + \frac{\partial^2 u(x,y,t)}{\partial y^2} \right), \quad (3)$$

where, $v_0 \in \mathbb{R}_+$ is the thermal diffusivity. As a movement law for prey, (3) models the case where there is no predator-prey interaction. The prey diffuses from its initial density, $u(x,y,0)$, at a ‘‘speed’’ of v_0 , regardless of the location of the predator front. The diffusion of the prey is shown as contour levels in Fig. 3.

Recall that an application for our work is mine clearing by teams of forging robots. Equation (3) captures the movement of objects like floating mines, as opposed to advanced mines (for details see [14]). The reaction-diffusion process described next, models the movement of more sophisticated threats, such as UUVs that react to the location of the foraging robots.

B. Reaction-diffusion

A reaction-diffusion process is a more natural representation of the prey movement than a simple diffusion process (as the one used in the previous subsection) since it incorporates the prey response to a predator charge. In general, a reaction-diffusion process models the changes in a substance under: 1) reaction - the influence of another substance and 2) diffusion - the spatial distribution. There are numerous mathematical models of a reaction-diffusion process and the one we use is known as the FitzHugh-Nagumo model. Because of its simplicity, this model is widely used in the field of mathematical biology to describe the firing of neurons and the propagation of nerve action potentials under the excitation of ion movement across a membrane [15]. We tailor the system of partial differential equations used to describe the FitzHugh-Nagumo model in [15] to model the propagation of prey under the excitement of the predator front as follows:

$$\frac{\partial u}{\partial t} = v(p(x,y)) \left(\frac{\partial^2 u}{\partial x^2} + \frac{\partial^2 u}{\partial y^2} \right) - \sigma p(x,y), \quad (4)$$

where $\sigma \in \mathbb{R}_+$ and the diffusion coefficient, v , now depends on the predator location, $p(x,y)$. For a curve $C(K)$, we define the predator location as follows:

$$p(x,y) = \begin{cases} 1 & \text{if } (x,y) \text{ on } C(K) \\ 0 & \text{otherwise} \end{cases}, \quad i \in \{1, \dots, M\}. \quad (5)$$

The diffusion coefficient is modeled as

$$v(p) = \begin{cases} v_0 + \kappa & \text{if } p = 1 \\ v_0 & \text{otherwise} \end{cases} \quad (6)$$

where $\kappa \in \mathbb{R}_+$. Such a formulation for the thermal diffusivity captures the idea of the prey being ‘‘scared’’ in the presence of predators. For a location (x,y) , when $p = 0$ (i.e., there are no predators present in that location), the prey-flock diffuses according to the nominal ‘‘speed’’ of v_0 ; but when $p = 1$, they diffuse faster at a speed of $v_0 + \kappa$. We also capture the idea of prey being ‘‘eaten’’ with the $-\sigma p$ term.

Our mathematical models for predator fronts and prey aggregations are based on creating simple, yet rich biological models. Recall that the goal of the work is not biomimicry, but to draw inspiration from biology for engineering applications. Next, based on our models of the predator front and the PDE-based models of prey movement, we characterize the optimal charging front in both the free lunch and no-free-lunch cases.

V. FRONT DESIGN

The most efficient charging front for a given feeding strategy is obtained through the solution to an optimization problem. From the set of candidate curves, \mathcal{C} , defined in Section III, the free-lunch curve maximizes the total energy intake of the foraging group and the no-free lunch curve maximizes the energy intake of the agent that feeds the least. But before we begin, we need to define the energy intake for an individual agent. If the position of agent i is denoted as $C_i(K)$ and we let agent i ‘‘eat’’ $u(C_i(K), t)$ amount of prey at time t , then the total amount of energy consumed, i.e. prey captured, by agent i is given by

$$E_i = \int_0^{t_f} u(C_i(K), t) dt, \quad i \in \{1, \dots, M\}. \quad (7)$$

With this definition of individual energy intake, we now characterize the optimal charging curves for the free lunch and the no-free lunch case.

Lions earn a free lunch by eating the prey caught by the more skilled hunters that take positions in the center of the front. In this case, the goal is to capture as much prey as possible for a group feasting to take place. Thus, since the total energy, E , is given by

$$E = \sum_{i=1}^M E_i, \quad (8)$$

the free lunch curve is the curve $C(K^*)$, where

$$K^* = \arg \max_K E \quad (9)$$

As opposed to lions, each dolphin in the foraging group must contribute in the hunt and as a result, in our formulation,

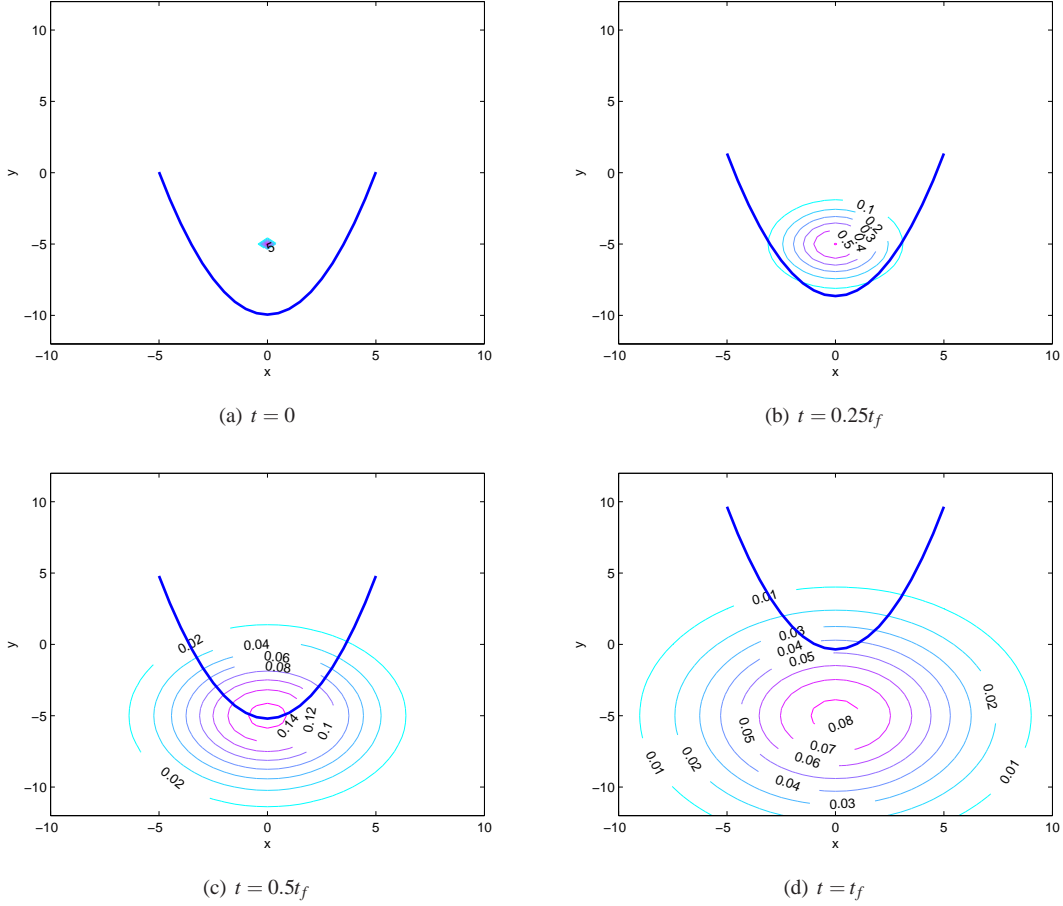


Fig. 3. The curve $C(-10)$ is sweeping through the prey (represented as contour levels), which are diffusing according to (3).

the no-free lunch curve is the curve that maximizes the total energy intake of the agent that feeds the least. Let the energy of the agent that feeds the least be denoted as E' , then

$$E' = \min_i E_i, \quad (10)$$

where $i \in \{1, \dots, M\}$. The no-free lunch curve is the curve $C(K')$, where

$$K' = \arg \max_K E' \quad (11)$$

VI. SIMULATIONS

The results of our model are shown in Fig. 4. The foraging area is represented as a 2D mesh, where $x_{min} = -30$, $x_{max} = 30$, $y_{min} = -30$, $y_{max} = 30$, and the mesh spacing is $\Delta x = \Delta y = 0.5$. The curves are swept from $t_i = 0$ to $t_f = 20$, with a time step of $\Delta t = 0.005$. The candidate curves are the curves between $K_i = -10$ and $K_f = 10$, with a step of $\Delta K = 0.5$ and arc length $L = 23$. We use 21 predator agents, thus curves are drawn using $M = 21$ equally-spaced data points.

Three distinct initial prey densities are considered. Each initial density is a ball of radius 4 units and they differ in the location of their center (denoted as ‘x’). In Figs. 4a and 4b, the center is located at $(0, -5)$; in Figs. 4c and 4d, the center is located at $(0, 0)$; and in Figs. 4e and 4f, the center

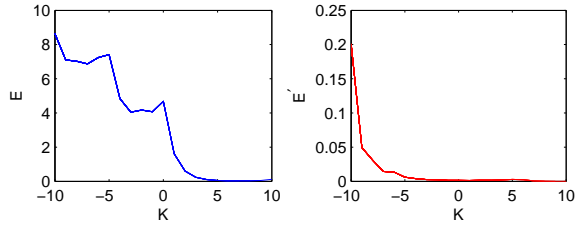
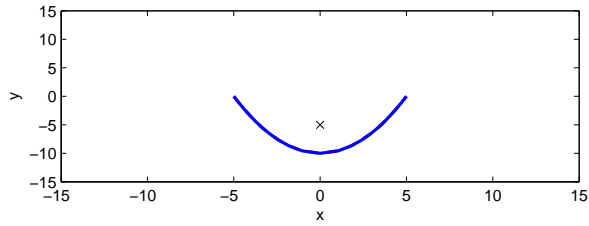
is located at $(0, 10)$. For each position, we simulate the prey movement as a diffusion process in Figs. 4a, 4c, and 4e; as a reaction-diffusion process in Figs. 4b, 4d, and 4f. The diffusion process parameters are $\nu_0 = 0.5$, $\kappa = \nu_0$, and $\sigma = 10$.

There are two curves displayed for each prey center of density and prey movement rule pair: the free lunch curve (solid line), which maximizes E , and the no-free lunch curve (dashed line), which maximizes E' .

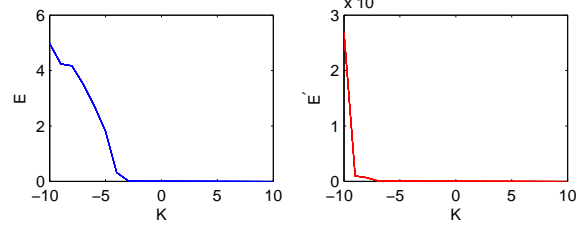
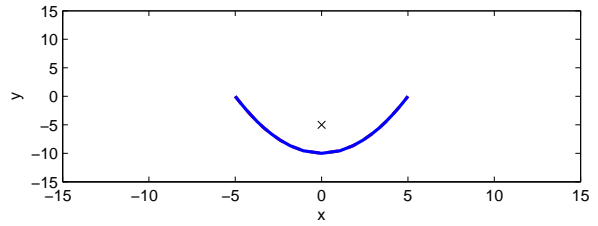
VII. DISCUSSION

Although we produced simple biological models of charging predator fronts, we observe that our simulations render strong resemblances to actual lion fronts (i.e., the free lunch case). In Figs. 4a, 4b, and 4d, we notice that our lion-inspired fronts look like the catcher’s mitt shape described in [2] - with agents in the wing and center positions.

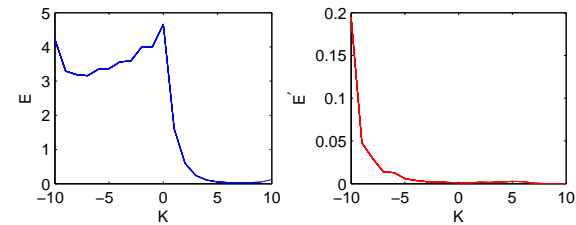
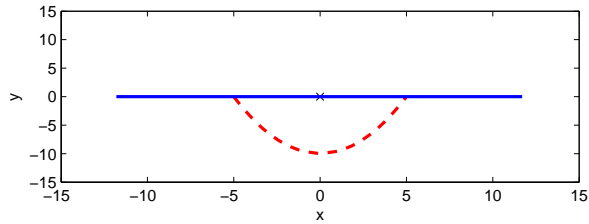
In the diffusion cases of Figs. 4c and 4e, the lion-inspired fronts are not U-shaped. This makes sense because in these cases, as opposed to the diffusion case of Fig. 4a, the candidate fronts sweep through more cells with a prey density value of 0. Thus, in these cases, to maximize E , the optimal curves are those that tend to “hug” the prey center and capture the most available prey at the start of the sweep.



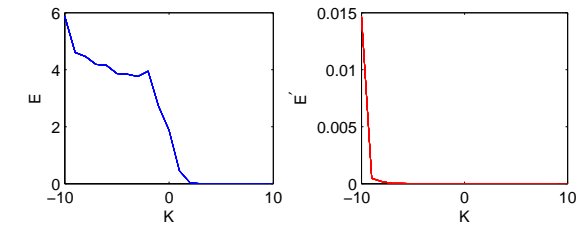
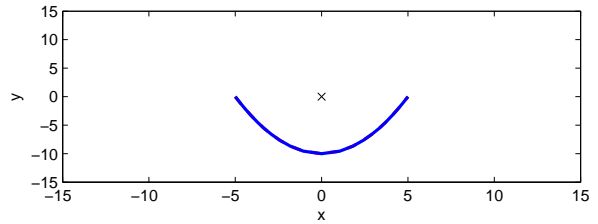
(a) Prey at (0,-5), $K^* = -10$, $K' = -10$



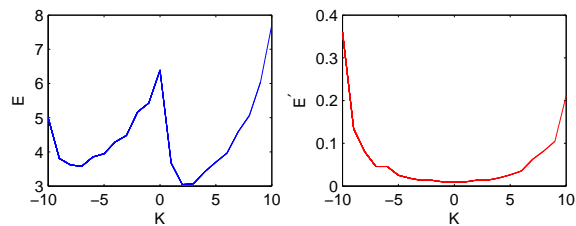
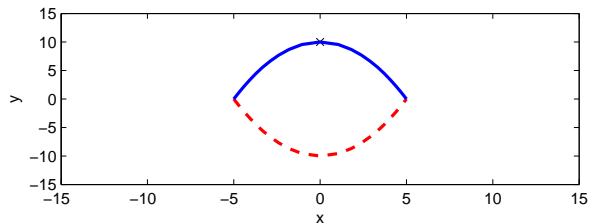
(b) Prey at (0,-5), $K^* = -10$, $K' = -10$



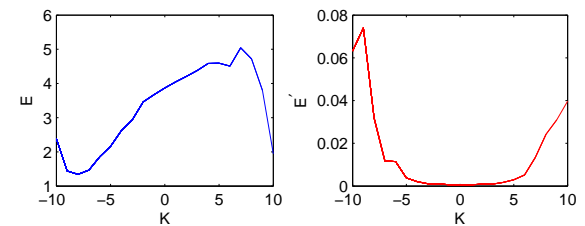
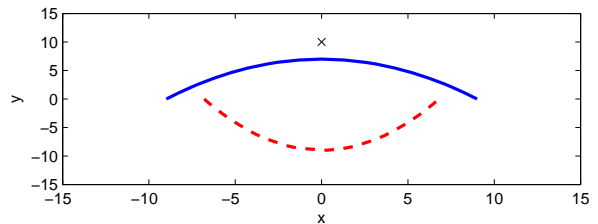
(c) Prey at (0,0), $K^* = 0$, $K' = -10$



(d) Prey at (0,0), $K^* = -10$, $K' = -10$



(e) Prey at (0,10), $K^* = 10$, $K' = -10$



(f) Prey at (0,10), $K^* = 7$, $K' = -8$

Fig. 4. *Left*: prey movement is modeled as a diffusion process. *Right*: prey movement is modeled as a reaction-diffusion process. The free lunch curve (solid line) and the no-free lunch curve (dashed line) is shown for different positions of the center of prey density ('x').

For the prey centered at $(0, -5)$, the lion-inspired fronts are the same for both the diffusion (Fig. 4a) and the reaction-diffusion case (Fig. 4b). However, we obtain different shapes for the diffusion and reaction-diffusion cases when the prey is centered at $(0, 0)$ and $(0, 10)$. As we mentioned earlier, in Figs. 4c and 4e, the optimal fronts are the ones that pass through the center of the prey at the beginning of the sweep. However, since our reaction-diffusion process models prey being scared, it turns out that the optimal thing to do is no longer to start the sweep as a curve that intersects the prey center. If the fronts begin the sweep by hugging the prey, they scare away a lot of the prey and there are fewer left to capture during the rest of the sweep. As a result, the optimal lion-like fronts during a reaction-diffusion case are less aggressive and tend to hold back more than their diffusion case counterparts. In the case of Fig. 4b, the curve cannot “avoid” the prey any longer than its counterpart of the diffusion case, since the optimal curve in the diffusion case is already the curve that holds back the most, $C(-10)$ (see Fig. 4a).

In the case of the dolphin-inspired predator fronts, we notice that the optimal curve is always the curve that can place the predators in the “wing” positions (which capture the least prey) in the path of the initial ball of prey density. Fig. 4f illustrates the only case when the optimal dolphin-like curve is not the curve $C(-10)$; in fact, the optimal curve is $C(-8)$ curve. This makes sense because this is a reaction-diffusion case and by the time a curve reaches the prey center, the prey have extensively diffused and as a result, to eat more, the predators in the wing positions must spread out further. The result is a more straightened version of the diffusion counterpart obtained in Fig. 4e.

Due to the simplified models of prey response and constant length requirements placed on the predator fronts, we cannot expect exact replicas of natural systems. Even though our goal is bioinspiration, as mentioned before, we observe strong biomimicry for the case of the lion-inspired fronts. Dolphins in the wall method tend to charge in a straight line and this is not obtained in our simulations. We do however capture one interesting difference between lions and dolphins: the fact that lions rely on stalking their prey and dolphins do not. The maximum speed a lions can attain is 48 – 59 Km/h, but they can only sustain this speed for a short distance [2]. The type of prey they hunt can usually outrun them and as a result, lions stalk their prey and charge only when they are within 30 m of their prey. On the other hand, dolphins tend to “drive” towards their for long distances (often until their drive is obstructed by the shore or boating activities [1]). This is captured by our results since the optimal lion-like fronts start in positions that are either the same distance or distance closer to the prey than the dolphin-like fronts.

VIII. CONCLUSIONS

During group hunting, Bottlenose dolphins and African lions arrange themselves to form a predator front that charges towards the aggregation of prey in unison. However, the

shape of the dolphin front is different from that of lions and this difference stems from the nature of the feeding strategy. We modeled the predator fronts as quadratic curves and used curve deformation techniques to characterize the most efficient curve for a given feeding strategy. With engineering applications as a possible back-end of our bio-inspired work, simple mathematical models of the predator charge were developed. However, these simple biological models were rich enough to capture the true shape of lion fronts with the inclusion of predator-prey interactions.

REFERENCES

- [1] K. Pryor and K. Norris, *Dolphin Societies*, University of California Press, Berkeley, CA; 1998.
- [2] R.D. Estes, *Behavior Guide to African Mammals*, University of California Press, Berkeley, CA; 1991.
- [3] *Autonomous Vehicles in Support of Naval Operations*, The National Academic Press, Washington D.C.; 2005.
- [4] D.A. Shell and M.J. Mataric, “On foraging strategies for large-scale multi-robot systems”, *Intl. Conf. on Intelligent Robots and Systems*, 2006, pp. 2717–2723.
- [5] T. Balch, “The impact of diversity on performance in multi-robot foraging”, *Proc. Third Conf. on Autonomous Agents*, 1999, pp. 92–99.
- [6] T.H. Labella, M. Dorigo, and J. Deneubourg, Self-organised task allocation in a group of robots, *Distributed Autonomous Robotic Systems*, 2004.
- [7] N. Lemmens, S. Jong, K. Tuyls, and A. Nowé, “Bee Behaviour in Multi-agent Systems”, *Adaptive Agents and Multi-Agent Systems III. Adaptation and Multi-Agent Learning*, 2008, pp. 145–156.
- [8] G. Ferrari-Trecate, M. Egerstedt, A. Buffa and M. Ji, Laplacian Sheep: A Hybrid, Stop-Go Policy for Leader-Based Containment Control, *Hybrid Systems: Computation and Control*, Springer-Verlag, 2006, pp. 212–226.
- [9] C. Packer and A.E. Pusey, Divided We Fall: Cooperation among Lions, *Scientific American Magazine*, May 1997.
- [10] F. Zhang, D.M. Fratantoni, D. Paley, J. Lund, and N.E. Leonard, Control of Coordinated Patterns for Ocean Sampling, *International Journal of Control*, vol. 80, No. 7, July 2007, pp. 1186–1199.
- [11] S. Lankton, D. Nain, A. Yezzi, and A. Tannenbaum, “Hybrid Geodesic Region-Based Curve Evolutions for Image Segmentation”, *SPIE Medical Imaging*, 2007.
- [12] S.-H. Lee, H.K. Pak, and T.-S. Chon, Dynamics of prey-flock escaping behavior in response to predator’s attack, *Journal of Theoretical Biology*, vol. 240, 2006, pp. 250–259.
- [13] M.A. Haque, A.R. Rahmani, and M. Egerstedt, “A Hybrid, Multi-Agent Model of Foraging Bottlenose Dolphins”, *Third IFAC Conf. on Analysis and Design of Hybrid Systems*, Zaragoza, Spain, 2009.
- [14] J.E. Rhodes and G.S. Holder, *Concept for Future Naval Mine Countermeasures in Littoral Power Projection*; 1998.
- [15] J.D. Murray, *Mathematical Biology I: An Introduction*, Springer, New York, NY; 2002.
- [16] R. Heinsohn and C. Packer, Complex Cooperative Strategies in Group-Territorial African Lions, *Science*, vol. 269, September 1995, pp. 1260–1262.